JOURNAL OF OPTOELECTRONICS AND ADVANCED MATERIALS Vol. 9, No. 7, July 2007, p. 2166 - 2169

The study of the influence of Al and Sn doping on the optical and electrical properties of ZnO thin films

P. PREPELITA, C. BABAN, F. IACOMI
Al.I. Cuza University, Faculty of Physics, 11 Carol I Blvd., 700506, Iasi Romania, iacomi@uaic.ro

ZnO thin films on glass substrates were obtained by thermal oxidation of vacuum evaporated Zn films. The evaporated metalic films with Al/Zn, Sn/Zn and (Al+Sn)/Zn in different weight ratios were annealed for 2 h at 450^{o}C to obtain Al-doped, Sn-doped and Al+Sn–doped ZnO films. The optical properties, evaluated by UV-VIS (350-1300 nm) showed that the obtained thin films were highly transparent, with a transmission coefficient between 65 – 90 % depending on the dopant type and the ammount of doping. For the same ammount of doping the electrical resistivity of Al doped films is lower than for Sn doped films but in both cases it is higher than the electrical resistivity of Al, Sn - doped films.

(Received March 4, 2007; accepted June 27, 2007)

Keywords: ZnO, thin films, TCO, doping

1. Introduction

Zinc Oxide (ZnO) is intensively investigated due to its intresting properties (high electrical conductivity, direct optical band-gap, high transmission in visible domain, wide band-gap energy, etc) and important applications like transparent conducting electrodes and buffer layers in sollar cell technology or as a material in sensor technology [1-4].

As a transparent conducting oxide (TCO) ZnO has the advantage of a lower cost than ITO but also has the disadvantage of instability in atmosphere and a large change of electrical resistance with temperature [5].

Another advantage is that ZnO films can be easily prepared through varous methods like sputtering [6,7], pulsed laser deposition [8,9], electrodeposition [10], chemical methods (spray pirolysis [11,12], spin-coating [13]) etc.

The properties of ZnO thin films are determined mainly by the non-stoichiometry of the films resulting from the presesence of oxygen vacancies and interstitial zinc. The electrical properties of ZnO films are also improved by doping [1-4,6,7,11,14,15] with different metals, the most studied case being of Al doped ZnO films (AZO).

In this paper optical and electrical properties of both doped (Al, Sn) and undoped ZnO thin films, prepared by thermal oxidation of metallic films, are investigated.

2. Experimental

ZnO thin films were prepared by thermal oxidation of metalic Zn films deposited onto properly cleaned glass substrates by vacuum evaporation. The thermal treatment was performed in air for two hours at 450^{o}C. For Al and Sn doped films we prepared first Al/Zn and Sn/Zn metalic films with weight ratios of 0.03 and 0.1.The films were then oxidised in air by following the same thermal treatment as for undoped films Doped thin films were also prepared from oxidised (Al+Sn)/Zn metalic films with 0.03 weight ratio. After the heat treatment the films became transparent.

The crystalline structure and surface morphology of doped and undoped ZnO thin films was investigated by means of X-ray diffraction (using a DRON-2 diffractometer with CoK_{α} radiation) and atomic force microscopy (AFM) respectively.

Transmission spectra, in the spectral range 350-1300 nm, were recorded using an UV–VIS (C. Zeiss, Jena) spectrophotometer. The band gap energy was calculated from absorbtion spectra.

The temperature dependence of the electrical conductivity was investigated using surface-type cells. Indium films were used as electrodes. They were deposited onto the substrates (by thermal evaporation under vacuum) after the preparation of doped and undoped ZnO films.

3. Results and discussion

XRD patterns show (Fig.1) that after annealing in air, doped and undoped ZnO films have a wurtzite (hexagonal) structure. Doped films have a preferential orientation with (002) planes parallel to the substrate. By increasing of the ammount of doping, the preferential orientation is reduced. XRD patterns also indicate changes in the peak intensities depending on the nature and the ammount of dopant.

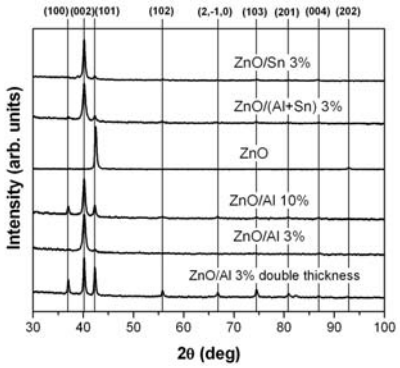

Fig. 1. XRD patterns for doped and undoped ZnO thin films.

No separate Zn phase was detected in XRD patterns indicating that the films were fully oxidised after the heat treatment.

Making the asumption that the peak broadening is determined only by the effect of crystallite size, the average crystallite size, *D*, can be calculated using the Debye -Scherrer expression [16].

$$D = \frac{0.9\lambda}{\beta \cos\theta} \qquad (1)$$

where λ =1.7889 Å is the wavelength of CoKα radiation, β denotes the full-width at haft-maximum of the peak and θ is the Bragg angle. The crystallite sizes calculated with eq. (1) are indicated in Table I.

The unit cell parameters were calculated considering the interplanar spacing for the hexagonal system, given by [16]

$$d_{hkl} = \left(\frac{4}{3} \frac{h^2 + hk + k^2}{a^2} + \frac{l^2}{c^2} \right)^{-1/2}, \qquad (2)$$

where *h*, *k*, *l* are Miller indices and *a* and *c* are the parameters of the unit cell. The unit cell parameters are listed in Table I. As can be observed from Table I the *c* parameter increases for doped films as compared with undoped ZnO films indicating the incorporation of the dopants by substitution in the host lattice.

Table 1. The unit cell parameters and crystallite sizes determined from XRD patterns(a, c – unit cell parameters, V – unit cell volume, D - average crystallite size).

Sample	*a* (nm)	*c* (nm)	*V*(nm^3)	*c*/*a*	*D* (nm)
ZnO/Al 10%	0.3256	0.5214	0.0479	1.601	20.9
ZnO/Al 3%	0.3253	0.5212	0.0477	1.602	16.4
ZnO/Sn 10%	0.3244	0.5211	0.04750	1.606	24.0
ZnO/Sn 3%	0.3258	0.5212	0.04792	1.600	22.9
ZnO/(Al+Sn) 3%	0.3255	0.5214	0.04783	1.602	17.9
ZnO	0.3248	0.5208	0.04759	1.603	24.5

Surface morphology investigated by AFM indicates (Fig. 2 a, b) that the surface is smooth and for all samples the roughness is of nm order. The surface roughness is influenced by the dopant nature and content. The effect of doping consists in a smoother surface and smaller grains. Thin films doped with Al are smoother and have smaller grains as compared with samples doped with Sn ($RMS_{Al3\%}$ = 7.8nm; $RMS_{Sn3\%}$ = 24.9 nm) and thin films doped with Sn and Al ($RMS_{(Al+Sn)\ 3\%}$ = 9.68 nm).

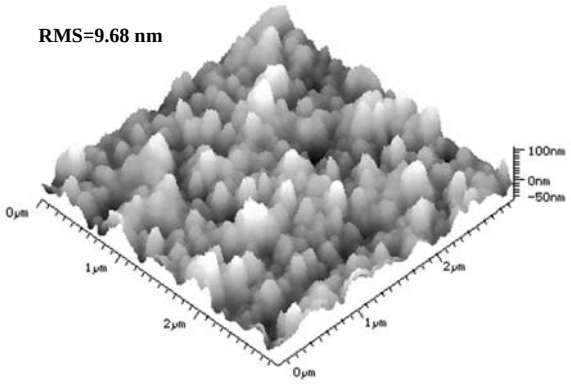

Fig. 2a: AFM image for ZnO/Sn 3% thin film

All investigated samples are highly transparent, with a transmission coefficient between 65 % and 90 % in the spectral range 500–1300 nm, for both doped and undoped films (Fig.3).

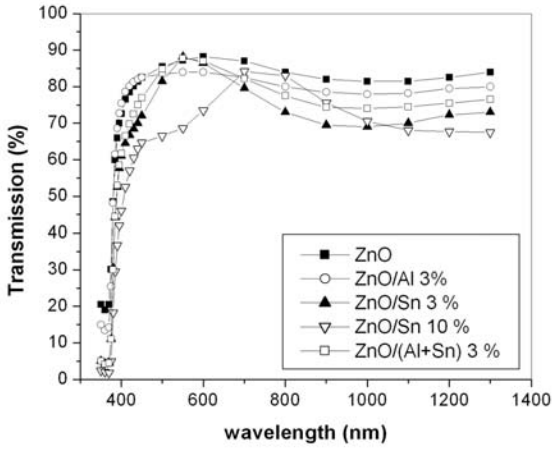

Fig. 3. Transmission spectra for doped and undoped ZnO thin films.

The absorption coefficient was calculated from the transmission spectra using the equation [17]

$$\alpha = \frac{1}{d} \ln \left[\frac{(1 - R_\lambda)^2}{T_\lambda} \right] \qquad (3)$$

where d denotes the film thickness, and R_λ and T_λ are reflection and transmission coefficient, respectively, at wavelength λ.

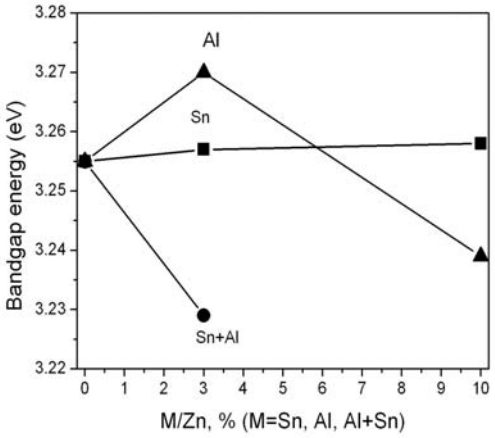

Fig. 4. Bandgap energy dependence on the ammount of doping and dopant type.

Above the fundamental absorption edge, for allowed direct transitions, the dependence of the absorption coefficient on the incident photon energy, $h\nu$, is given by [17]

$$\alpha h\nu = A\left(h\nu - Eg\right)^{1/2} \quad (4)$$

with Eg representing the energy bandgap while A is a characteristic parameter independent of photon energy. According to (3), $(\alpha h\nu)^2$ linearly depends on the photon energy, $h\nu$. The values of bandgap are determined by extrapolating the linear portions to $(\alpha h\nu)^2 = 0$. The values of the bandgap energy and its dependence on the dopant type and the ammount of doping is indicated in Fig. 4. Al doping have a more pronounced influence on the bandgap energy of the films as compared with Sn doping. While for ZnO/Al 3% and ZnO/Sn 3% films the bandgap energy is increasing for ZnO/(Al + Sn) 3% doped films the bandgap energy is decreasing giving the same effect as for ZnO/Al 10% doped films.

The electrical resistivity for doped and undoped ZnO films, at room temperature, is presented in Fig. 5. It can be observed that for Al doped ZnO films there is an optimal doping arround 3%. For higher ammount of doping the electrical resistivity is increasing from 0.1 Ωcm to 0.28 Ωcm. The same effect is observed also for Sn doped ZnO films the resistivity increasing from 0.15 Ωcm to 0.30 Ωcm. In this case the resistivity is higher than in the case of Al doping.

Instead, doping with Al and Sn gives a lower value for the electrical resistivity, 0.05 Ωcm.

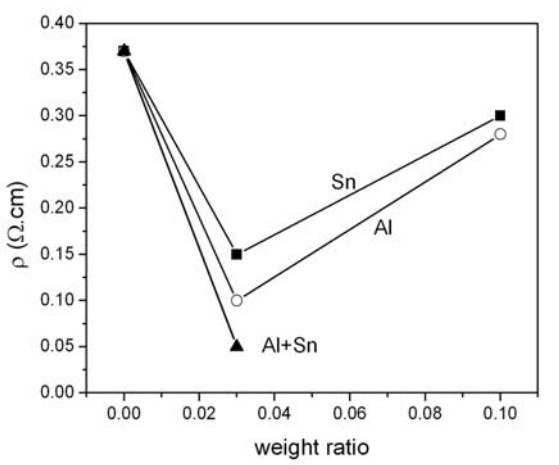

Fig. 5. Electrical resistivity at room temperature for doped and undoped ZnO thin films.

Although the grain sizes increase for higher ammounts of dopant the increasing of the resistivity may be caused by the segregation of the dopant at grain boundaries [18].

The temperature dependence of the electrical conductivity is typical as for semiconducting materials. The activation energy of electrical conduction in the temperature range between room temperature and 150°C was found to be 81 meV for ZnO/Sn 3% films, 33 meV for ZnO/Al 3% and 59 meV for ZnO/(Al+Sn) 3%.

4. Conclusion

By thermal oxidation of metallic Zn films we prepared highly transparent and conductive ZnO films with good adherence on the substrates and smoot surfaces. The structure of doped films is hexagonal with a prefferential (002) orientation. The crystallinity, optical and electrical properties of the samples are influenced by the dopant type and content. We have found that the Al + Sn doping enhances the electrical properties as compared with the same ammount of doping using only one element.

References

[1] S. J. Pearton, D. P. Norton, K. Ip, Y. W. Heo, T. Steiner, Superlattices and Microstructures **34**, 3 (2003).
[2] W. J. Jeong, S. K. Kim, G. C. Park, Thin Solid Films, **506-507**, 180 (2006).
[3] J. Müller, B. Rech, J. Springer, M. Vanecek, Solar Energy, **77**, 917 (2004).
[4] H. Gong, J. Q. Hu, J. H. Wang, C. H. Ong, F. R. Zhu, Sensors and Actuators B, **115**, 247 (2006).
[5] D. Shimono, S. Tanaka, T. Torikai, T. Watari, M. Muranoa, Journal of Ceramic Processing Research, **2**, 184 (2001).

[6] K. H. Kim, R. A. Wibowo, B. Munir Materials Letters, **60**, 1931 (2006).
[7] Oliver Kluth, Gunnar Schöpe, Bernd Rech, Richard Menner, Mike Oertel, Kay Orgassa and Hans Werner Schock, Thin Solid Films **502**, 311 (2006).
[8] A. Og. Dikovska, P. A. Atanasov, C. Vasilev, I. G. Dimitrov, T. R. Stoyanchov, J. Optoelectron. Adv. Mater. **7**, 1329 (2005).
[9] Yolanda Y. Villanueva, Da-Ren Liu and Pei Tzu Cheng, Thin Solid Films **501**, 366 (2006).
[10] R. E. Marotti, P. Giorgi, G. Machado and E.A. Dalchiele, Sol. Energ. Mat. Sol. C. **90**, 2356 (2006).
[11] M. A.Lucio-López, M. A. Luna-Arias, A. Maldonado, M. de la L. Olvera, D. R. Acosta, Sol. Energ. Mat. Sol. C. **90**, 733 (2006).
[12] C. Gümüş, O. M. Ozkendir, H. Kavak, Y. Ufuktepe, J. Optoelectron. Adv. Mat., **8**, 299 (2006).
[13] B. J Norris, J Anderson, J. F. Wager, D A Keszler, J. Phys. D: Appl. Phys. **36**, L105 (2003).
[14] K. Ellmer, J. Phys. D: Appl. Phys. **33**, R17 (2000).
[15] B. G. Choi, I. H. Kim, D. H Kim, K. S. Lee, T.S. Lee, B. Cheong, Y.-J. Baik, W.M. Kim, Journal of the European Ceramic Society, 25 (2005) 2161.
[16] B. D. Culity, Elements of X-Ray Diffraction, Addison-Wesley (1978) 356
[17] J. N. Hodgson, Optical Absorbtion and Dispersion in Solids, Chapman & Hall, London (1970).
[18]B. J. Ingram, G. B. Gonzalez, D. R. Kammler, M. I. Bertoni, T. O. Mason, Journal of Electroceramics, **13**, 167 (2004).

*Corresponding author: prepelitapetro@yahoo.co.uk